nature nanotechnology

LETTERS

PUBLISHED ONLINE: 2 NOVEMBER 2014 | DOI: 10.1038/NNANO.2014.243

Feedback-driven self-assembly of symmetry-breaking optical metamaterials in solution

Sui Yang[1,2], Xingjie Ni[1], Xiaobo Yin[1,2], Boubacar Kante[1], Peng Zhang[1], Jia Zhu[1], Yuan Wang[1,2] and Xiang Zhang[1,2,3,4]*

Thermodynamically driven self-assembly offers a direct route to organize individual nanoscopic components into three-dimensional structures over a large scale[1–3]. The most thermodynamically favourable configurations, however, may not be ideal for some applications. In plasmonics, for instance, nanophotonic constructs with non-trivial broken symmetries can display optical properties of interest, such as Fano resonance, but are usually not thermodynamically favoured[4]. Here, we present a self-assembly route with a feedback mechanism for the bottom-up synthesis of a new class of symmetry-breaking optical metamaterials. We self-assemble plasmonic nanorod dimers with a longitudinal offset that determines the degree of symmetry breaking and its electromagnetic response. The clear difference in plasmonic resonance profiles of nanorod dimers in different configurations enables high spectra selectivity. On the basis of this plasmonic signature, our self-assembly route with feedback mechanism promotes the assembly of desired metamaterial structures through selective excitation and photothermal disassembly of unwanted assemblies in solution. In this fashion, our method can selectively reconfigure and homogenize the properties of the dimer, leading to highly monodispersed aqueous metamaterials with tailored symmetries and electromagnetic responses.

In the last decade, control over structural symmetries has led to novel materials properties and the prediction of potentially exciting applications. Optical metamaterials[5], unlike conventional materials, can be designed to have negative refraction, rainbow trapping and nonlinear metal optics. However, particularly rich and exciting physics comes into play when symmetry-breaking mechanisms are introduced that have the potential to enable strong anisotropic plasmon hybridization[6], leading to unusual phenomena including plasmon-induced transparency[7], anti-Hermitian plasmonic antennas[8] and optical magnetism, and consequently negative-index metamaterials[9]. These intriguing properties can be used in a number of important applications, such as subwavelength imaging, optical cloaking and sensing[10–12].

These applications could be hindered by the fact that most structures are fabricated predominantly by top-down lithography, a technique that is inefficient for producing isotropic metamaterials in three dimensions and is often not cost-effective for large-scale fabrication. To mitigate these limitations, self-assembly approaches have recently been explored. However, they generate the most thermodynamically favourable structure, which usually results in a high degree of structural symmetry and inevitable inhomogeneity. For example, such self-assembly methods have been used to synthesize symmetric coupled plasmonic nanoclusters on a substrate[13]. Very recently, assisted by DNA or polystyrene-particle scaffolds, a circular dichroic plasmonic cluster and optical metafluid with high symmetry have also been reported[14,15]. A significant challenge would be to overcome this thermodynamic restriction and assemble unconventional symmetry-breaking nano-entities with high structural uniformity. Accordingly, we have developed a self-assembly route with feedback that exploits the nanostructures' own optical properties and their responses to external light to reassemble with specific symmetry-breaking and optical properties. This unique feedback mechanism leads to precisely controlled nanostructures with beyond conventional symmetries and functionalities.

The assembly system we consider, as a demonstration, is a symmetry-breaking nanorod dimer, coupled side by side, with a longitudinal offset that defines the degree of symmetry breaking (Fig. 1). This offset endows the structure with anisotropically localized electromagnetic modes (Supplementary Fig. 1), leading to applications such as the plasmonic ruler[16], field-enhanced spectroscopy[4] and optical magnetism for negative-index metamaterials[17]. However, these asymmetrically coupled plasmonic structures are often not thermodynamically favourable, and the self-assembly of such structures remains a challenge. By judicious selection of linker molecules, the bonding direction of gold nanorods can be controlled to form directional nanodimers and, as has been demonstrated recently, chiral plasmonic structures[18]. Nevertheless, all previously reported nanorod assemblies, in general, tend to aggregate and align side by side or end to end as a consequence of maximized interparticle interaction and minimized surface energy, and there is no controlled structural selection with a longitudinal symmetry-breaking phenomenon[19–21].

To create the asymmetrically coupled metallic dimers with a longitudinal offset, we first synthesized colloidal gold nanorods with a seed-mediated growth method[22] and uniquely assembled the nanorods anisotropically at a water–chloroform interface (Fig. 1b). During synthesis, a bilayer of positive charged cetyltrimethylammonium bromide (CTAB) molecules was preferentially bonded along the longitudinal facets, stabilizing the growth of the nanorods with preferred crystal orientations[23]. The ligand-exchange process was subsequently applied to deactivate and partially replace the CTAB bilayer with the hydrophobic ligand octadecyltrimethoxysilane (ODS). By controlling the concentration of the hydrophobic ligands and the time of surface hydrophobication, we were able to stabilize the nanorods at the water–chloroform interface with partially decorated positive surfaces. When negatively charged spacer molecules (disodium chromoglycate, DSCG) were introduced, dimers formed electrostatically at the interface and an offset along the longitudinal side was created because the patched deactivation

[1]NSF Nano-scale Science and Engineering Center (NSEC), 3112 Etcheverry Hall, University of California at Berkeley, Berkeley, California 94720, USA, [2]Materials Sciences Division, Lawrence Berkeley National Laboratory, 1 Cyclotron Road, Berkeley, California 94720, USA, [3]Department of Physics, King Abdulaziz University, Jeddah, 21589, Saudi Arabia, [4]Kavli Energy NanoSciences Institute at the University of California, Berkeley, and Lawrence Berkeley National Laboratory, Berkeley, California 94704, USA. *e-mail: xiang@berkeley.edu

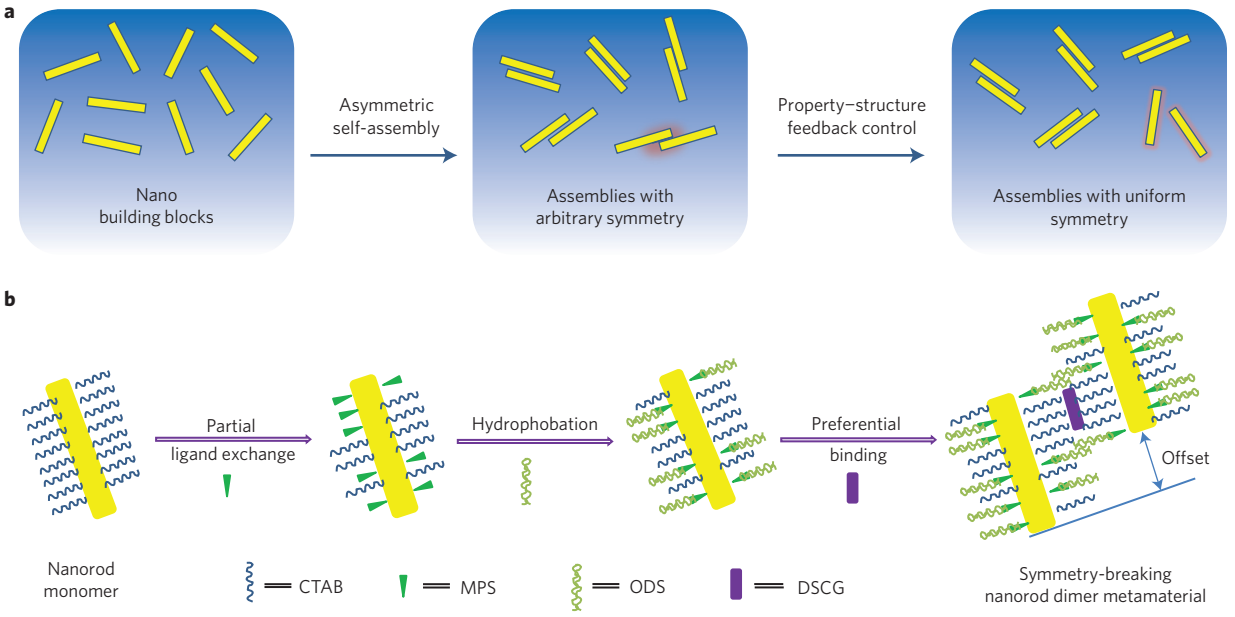

Figure 1 | Scheme of self-assembly route with self-corrected feedback mechanism mediated by the products' own properties. a, As an example, assembled entities with arbitrary symmetries, in particular broken symmetries, can be achieved using our self-assembly route to overcome thermodynamic limitations and achieve precise structural and symmetry control. **b**, Schematic of the preferential asymmetric binding technique. To assemble symmetry-breaking dimers, a gold nanorod monomer with cetyltrimethylammonium bromide (CTAB) coating was first modified via a partial ligand exchange process to prepare a chemically stable and patchy organosilane shell using mercaptopropyltrimethoxysilane (MPS) as a linker and octadecyltrimethoxysilane (ODS) as the hydrophobation agent. The space agent, disodium chromoglycate (DSCG), was then introduced to achieve electrostatic assembly. To maximize surface molecule interaction, two nanorods tend to align side by side, with an offset in the longitudinal direction.

sites of the two nanorods could not be generated symmetrically. The reduced growth rate due to surface hydrophobication and steric interactions[24,25] among ligands prevented the generation of side-by-side aggregates and stabilized the structure at the dimer stage (for details see Supplementary section 'Experimental method and characterization' and Supplementary Fig. 2).

Monomeric gold nanorods with an average aspect ratio of $\sim 3.2 \pm 0.2$ before assembly can be identified in the transmission electron microscopy (TEM) image in Fig. 2a, and the high-resolution TEM image in the inset to Fig. 2a reveals the longitudinal crystal facets to be {100}, the preferred high-affinity surface for CTAB bilayers[23]. After assembly, asymmetrically coupled nanorod pairs were formed parallel with the offsets (symmetry-breaking) along the longitudinal axis. Typical offsets were between 5 and 30 nm (Fig. 2b, Supplementary Fig. 3). The high-resolution TEM image in the inset to Fig. 2b shows a typical gap separation of ~5 nm (the blurred crystal surfaces of the dimers are mainly due to surface functionalization).

The optical scattering spectra and corresponding TEM images of an individual nanorod monomer (dimensions of 68×21 nm) show longitudinal surface plasmon resonances (λ_{max} at ~686 nm) due to the excitation of surface plasmon oscillation along the long axis of the monomer (Fig. 2c, Supplementary Fig. 4). The dimer, asymmetrically coupled by two nanorods with an offset of ~20 nm and a gap separation of ~5 nm, has an intriguing spectrum due to plasmon hybridization (Fig. 2d), where the hybridized modes are determined by the gap and mutual offset. The longitudinal plasmon resonance at ~694 nm is therefore regarded as the electric dipolar mode (symmetric plasmon coupling of the dimer), slightly redshifted as compared to that of the monomer. A relatively narrower peak at ~905 nm is also distinctly visible. This is a signature of the magnetic dipolar response from the antisymmetric plasmon coupling of the dimer (Fig. 2e), which is the key precursor for the formation of optical negative-index metamaterials.

Although this spectroscopic study of an individual symmetry-breaking dimer proves the magnetic property of metamaterials, the optical modes of the entire ensemble of as-assembled nanostructures might be smeared due to the intrinsic inhomogeneous broadening in a self-assembly system. It has been a fundamental challenge to obtain monodispersed aqueous assemblies with uniform structural symmetries and the desired ensemble optical properties. To address this issue, we developed a self-assembly and feedback mechanism that uses the structures' electromagnetic signature as a feedback to selectively reconfigure and homogenize ensemble nanoassemblies. Specifically, our process is based on the strong structural dependence of the plasmon resonance of gold nanorod dimers (which absorb light to a substantial extent[26]), which can be used selectively to break the weak electrostatic binding between gold nanorods via photothermal dissociation[27,28]. As shown schematically in Fig. 3a, plasmon excitation at the resonance frequency can be used in a selective way such that undesired assemblies are dissociated due to the photothermal effect while leaving desired (off-resonance) ones intact. Meanwhile, the released linker molecules could induce dimer recombination through an electrostatic interaction[29,30]. Under these conditions, dimers with the correct offset will be formed, because the laser irradiation prevents the growth of undesired dimers. By illuminating at designated wavelengths, the plasmonic nanorod dimer structures will be reshaped and remain at a given offset with uniformly controlled symmetry breaking.

Quantitative results of the structural reconfiguration and optical properties before and after self-assembly with selective plasmon feedback control are shown in Fig. 3. A broad distribution of dimer offsets is observed from the as-assembled dimer structures (Fig. 3b). The extinction spectrum of the assembly in solution shows the asymmetric broad longitudinal dipolar response that is the result of structural inhomogeneity (Fig. 3c). In contrast to the sharp and distinct magnetic resonances of the individual

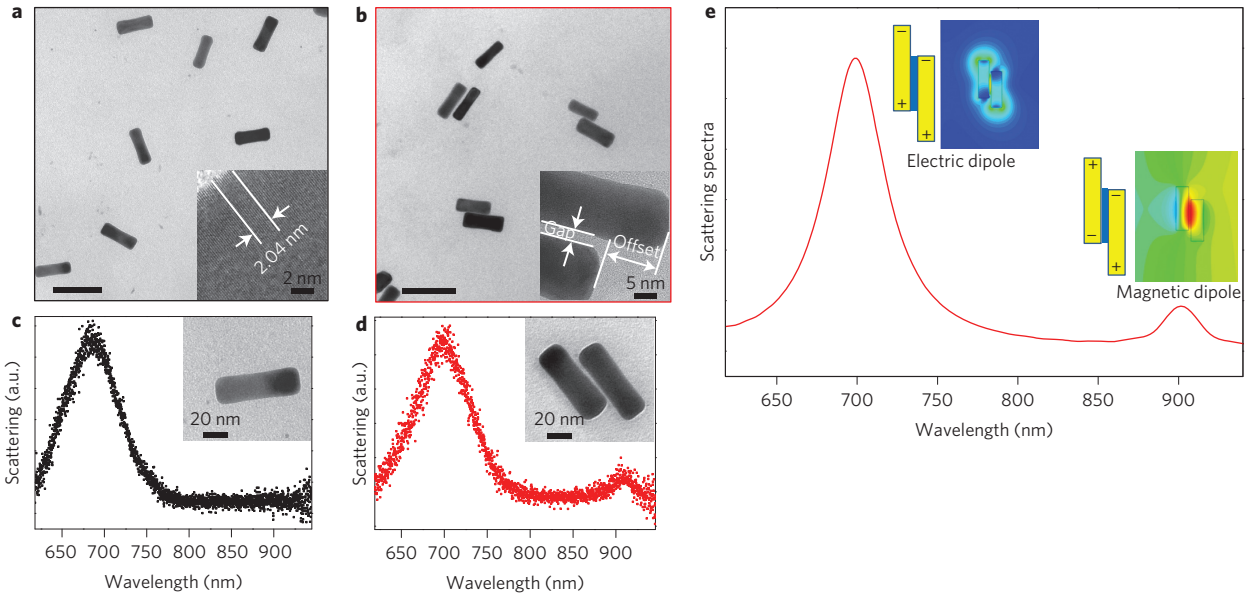

Figure 2 | Chemical assembly of optical metamaterials with symmetry breaking. a, TEM image of gold nanorod monomers, showing monodisperse and discrete nanorod building blocks due to positive charge repulsion. Inset: High-resolution TEM image showing crystal facets and fringes with a lattice spacing of 0.204 nm (2.04 nm in ten fringes) that can be indexed as the [100] plane of face-centred cubic (fcc) gold, with growth in the [001] direction. **b**, Symmetry-breaking dimers after assembly. Inset: High-resolution TEM image suggesting the typical gap separation and surface functionalization with a blurred edge. The offset is determined as shown. Scale bars in **a**,**b** (main panels), 100 nm. **c**,**d**, Dark-field scattering spectra (inset, TEM images) of individual nanorod monomer (**c**, black; 68 × 21 nm) and dimer (**d**, red; dimensions of nanorods, 68 × 22 nm, 71 × 20 nm; gap, 5 nm, offset, 20 nm). The magnetic dipolar mode around 905 nm (**d**) is clearly distinguished and can be described as a closed loop of nanoinductors and nanocapacitors between two asymmetrically coupled nanorod elements. **e**, Simulated far-field scattering spectrum of the corresponding symmetry-breaking dimer. Inset: Fields corresponding to each resonance peak: in-plane electric field (left) for the electric dipole; out-of-plane magnetic field (right) for magnetic dipole.

symmetry-breaking dimers shown in Fig. 2d, no observable magnetic dipole response can be distinguished because of intrinsic inhomogeneous broadening.

Evidence for the magnetic dipolar response can be observed in the spectra taken after quantitative structural reconfiguration with feedback control. In a typical experiment, a femtosecond laser was operated at a chosen wavelength to break the weak electrostatic interaction between the dimer elements, with an average power density of 0.875 kW cm^{-2} (much smaller than has been used to dissociate a covalent bond[27]). Figure 3d presents a statistical histogram of the ensemble structural distributions after laser irradiation from 760 nm to 930 nm. The distribution of offsets is pronounced at 10–20 nm and much improved compared to the as-assembled samples (Fig. 3b), indicating the effectiveness of the present selective structure homogenization (Supplementary Fig. 6). As is reflected in the optical extinction spectra of the aqueous ensemble, the previously broad and asymmetric response is now split into two narrow resonances at peak λ_{max} values of ~740 nm and ~960 nm (Fig. 3e). These can be ascribed to the collective ensemble longitudinal electric dipolar and magnetic dipolar modes, respectively, and conform well to our calculated results. The observed magnetic dipolar resonance emerges due to the annihilation of inhomogeneous broadening after self-assembly with selective structural feedback control. The difference in resonance frequencies arises due to the fact that they are in solution and on substrate, with different medium indices. The slightly wider resonance compared to the individual dimer spectrum (Fig. 2d) is attributed to the averaging effect over various orientations of dimers in solution by unpolarized excitation. It is worth noting that the electromagnetic properties we achieve here are fully isotropic in three dimensions, which is desirable and advantageous for the implementation of important metamaterial applications such as the fabrication of a perfect lens[10] and transformation optics[11].

To obtain the emerging metamaterial effective properties, we quantified the ensemble's magnetic dipole by measuring the angle- and polarization-resolved light scattering spectra (Fig. 4a). In this plot, the measured azimuth angular scattering pattern (red circles), the weighted combination of the electric (dashed cyan line) and magnetic (dashed magenta line) dipole radiations, indicates a substantial magnetic dipole contribution of 78%, which matches well with the calculation (solid blue line). By numerically extracting the averaged polarization and magnetization density, we successfully obtained the effective properties of our assembled aqueous symmetry-breaking metamaterials (Fig. 4b). As is shown, the optical properties of the metamaterials are highly tunable with filling factors. The effective metamaterial index is much smaller than the index of the water medium ($n = 1.33$) across all wavelengths, even at low filling factors of ~0.1. As the filling factor increases, it leads to isotropic negative-index optical metamaterials (for details see Supplementary Discussion 1 and Supplementary Figs 9 and 10).

To further demonstrate the capability of our method to control the level of symmetry breaking, we extended our synthesis of nanorod dimer colloidal metamaterials with another offset at ~20–30 nm. We again overcame the thermodynamic constraints using our self-assembly route with feedback, which led to uniform metamaterial structures and appreciable isotropic optical magnetic response. With this different level of symmetry breaking, we demonstrated a shift in the ensemble electric and magnetic dipolar resonances to 760 nm and 870 nm, respectively, which matches our simulation results well (for details see Supplementary Discussion 2 and Supplementary Figs 11–13).

In summary, we have demonstrated a self-assembly route with self-feedback mechanism to synthesize a new class of aqueous symmetry-breaking metamaterials with isotropic optical metamaterials properties. Our method could expand structural design

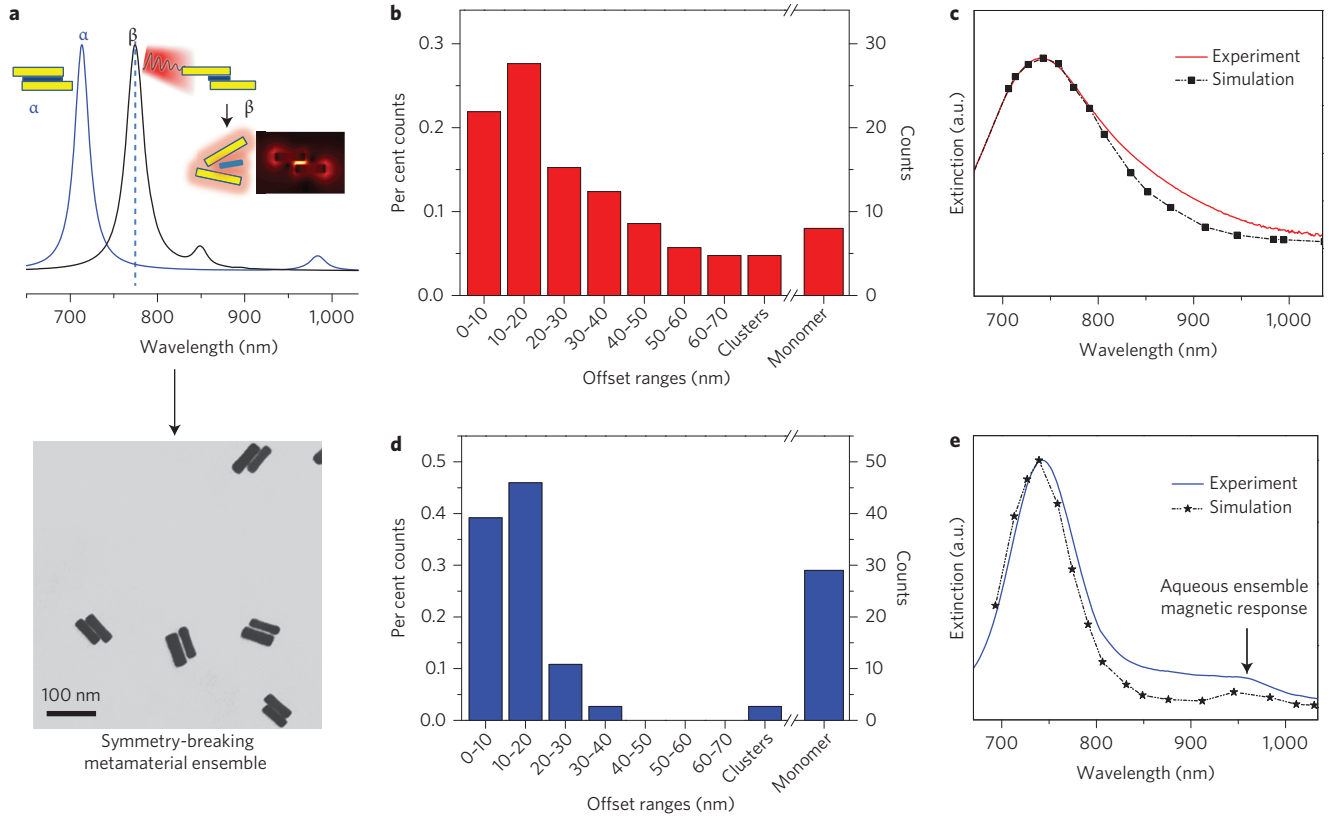

Figure 3 | Self-selective feedback assembly of symmetry-breaking metamaterial in which structural reconfiguration is mediated by its own plasmonic property. a, Mechanism of structural reconfiguration and symmetry selection. Under plasmon excitation at a selected wavelength, for example, the process works in such a way that the local heat generated by the photothermal effect dissociates incorrect structures β (optical field in the gap region is shown in the inset) while leaving the non-resonant, desired structure α intact. The resulting symmetry-breaking structure is shown in the TEM image with a pronounced homogeneous offset of ~10–20 nm. **b**,**c**, Statistical histogram (**b**) of as-assembled sample before structural feedback control, showing a wide variability of dimer offsets from an analysis of 114 particles, which experiences the intrinsic spectral inhomogeneous broadening shown in **c**. **d**, Particle distribution histogram of an ensemble of metamaterials after structural feedback control, indicating a striking redistribution of offsets with analysis of 104 particles. This indicates a uniform structure (offset pronounced at ~10–20 nm). The corresponding representative TEM image is shown in **a**. **e**, Experimental and simulated spectra for the ensemble of symmetry-breaking metamaterials after structural feedback control. Besides the characteristic electric dipolar resonance, a signature of magnetic dipolar peak becomes visible at ~960 nm and matches well with simulations. All responses are regarded as isotropic because there is no preferred structural orientation in the aqueous assembly.

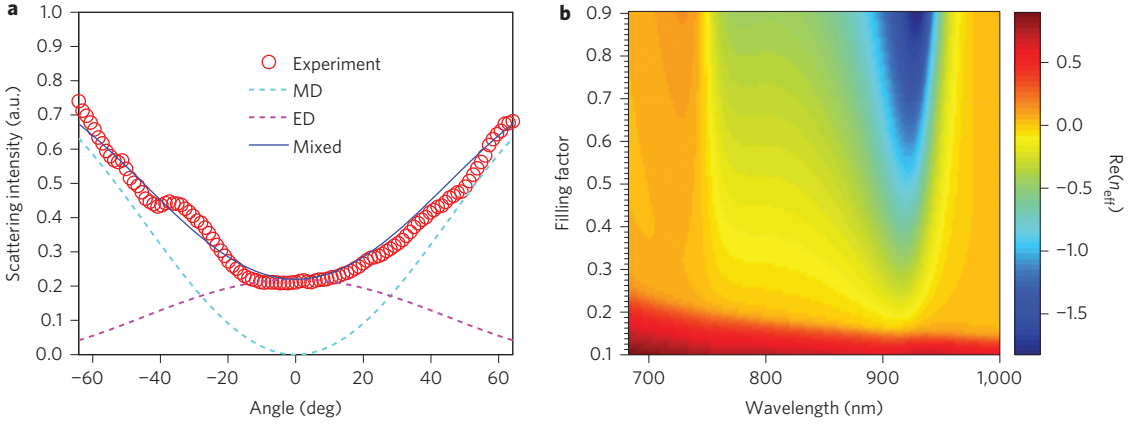

Figure 4 | Emerging metamaterial effective properties. a, Angle-resolved scattering pattern of the ensemble of symmetry-breaking nanorod dimer metamaterials. The dashed magenta and cyan curves shows the scattering patterns for magnetic (MD) and electric (ED) dipoles, respectively, with intensities of 78% and 22%. Red circles depict measured data at the magnetic resonance peak position in the sample. Data are averaged from ten different measurements in different sample positions. The solid blue line is a weighted combination of the electric and magnetic dipole radiations with the weight of the magnetic dipole radiation as the fitting parameter. **b**, Effective refractive index n_{eff} plotted as a function of filling factor and wavelength. The effective refractive index of the metamaterial becomes negative with increasing filling factors.

freedom and enrich the functionalities of artificial materials beyond typical thermodynamic limitations. The concept of self-assembly/disassembly mediated using the products' own properties as an autonomous feedback control may offer a drastically new perspective for the self-selective assembly of complex nanoarchitectures with tailored symmetry for applications previously deemed unfeasible. In contrast to the conventional wisdom that a material's structure determines its physical properties, we provocatively suggest that the final properties of materials, by design, may dictate the evolution of self-assembly and self-determine the final structure.

Received 23 January 2014; accepted 16 September 2014; published online 2 November 2014

References

1. Mann, S. & Ozin, G. A. Synthesis of inorganic materials with complex form. *Nature* **382,** 313–318 (1996).
2. Whitesides, G. M. & Grzybowski, B. Self-assembly at all scales. *Science* **295,** 2418–2421 (2002).
3. Shevchenko, E. V., Talapin, D. V., Kotov, N. A., O'Brien, S. & Murray, C. B. Structural diversity in binary nanoparticle superlattices. *Nature* **439,** 55–59 (2006).
4. Luk'yanchuk, B. *et al.* The Fano resonance in plasmonic nanostructures and metamaterials. *Nature Mater.* **9,** 707–715 (2010).
5. Shalaev, V. M. Optical negative-index metamaterials. *Nature Photon.* **1,** 41–48 (2007).
6. Prodan, E., Radloff, C., Halas, N. J. & Nordlander, P. A hybridization model for the plasmon response of complex nanostructures. *Science* **302,** 419–422 (2003).
7. Zhang, S., Genov, D. A., Wang, Y., Liu, M. & Zhang, X. Plasmon-induced transparency in metamaterials. *Phys. Rev. Lett.* **101,** 047401 (2008).
8. Zhang, S. *et al.* Anti-Hermitian plasmon coupling of an array of gold thin-film antennas for controlling light at the nanoscale. *Phys. Rev. Lett.* **109,** 193902 (2012).
9. Aydin, K., Pryce, I. M. & Atwater, H. A. Symmetry breaking and strong coupling in planar optical metamaterials. *Opt. Express* **18,** 13407–13417 (2010).
10. Pendry, J. B. Negative refraction makes a perfect lens. *Phys. Rev. Lett.* **85,** 3966–3969 (2000).
11. Pendry, J. B., Schurig, D. & Smith, D. R. Controlling electromagnetic fields. *Science* **312,** 1780–1782 (2006).
12. Liu, N. *et al.* Plasmonic analogue of electromagnetically induced transparency at the Drude damping limit. *Nature Mater.* **8,** 758–762 (2009).
13. Fan, J. A. *et al.* Self-assembled plasmonic nanoparticle clusters. *Science* **328,** 1135–1138 (2010).
14. Kuzyk, A. *et al.* DNA-based self-assembly of chiral plasmonic nanostructures with tailored optical response. *Nature* **483,** 311–314 (2012).
15. Sheikholeslami, S. N., Alaeian, H., Koh, A. L. & Dionne, J. A. A metafluid exhibiting strong optical magnetism. *Nano Lett.* **13,** 4137–4141 (2013).
16. Liu, N., Hentschel, M., Weiss, T., Alivisatos, A. P. & Giessen, H. Three-dimensional plasmon rulers. *Science* **332,** 1407–1410 (2011).
17. Kante, B., O'Brien, K., Niv, A., Yin, X. & Zhang, X. Proposed isotropic negative index in three-dimensional optical metamaterials. *Phys. Rev. B* **85,** 041103 (2012).
18. Ma, W. *et al.* Chiral plasmonics of self-assembled nanorod dimers. *Sci. Rep.* **3,** 1934 (2013).
19. Caswell, K. K., Wilson, J. N., Bunz, U. H. F. & Murphy, C. J. Preferential end-to-end assembly of gold nanorods by biotin–streptavidin connectors. *J. Am. Chem. Soc.* **125,** 13914–13915 (2003).
20. Huang, X., Neretina, S. & El-Sayed, M. A. Gold nanorods: from synthesis and properties to biological and biomedical applications. *Adv. Mater.* **21,** 4880–4910 (2009).
21. Vigderman, L., Khanal, B. P. & Zubarev, E. R. Functional gold nanorods: synthesis, self-assembly, and sensing applications. *Adv. Mater.* **24,** 4811–4841 (2012).
22. Nikoobakht, B. & El-Sayed, M. A. Preparation and growth mechanism of gold nanorods (NRs) using seed-mediated growth method. *Chem. Mater.* **15,** 1957–1962 (2003).
23. Murphy, C. J. *et al.* Anisotropic metal nanoparticles: synthesis, assembly, and optical applications. *J. Phys. Chem. B* **109,** 13857–13870 (2005).
24. Lin, Y., Skaff, H., Emrick, T., Dinsmore, A. D. & Russell, T. P. Nanoparticle assembly and transport at liquid–liquid interfaces. *Science* **299,** 226–229 (2003).
25. Grzelczak, M. *et al.* Steric hindrance induces crosslike self-assembly of gold nanodumbbells. *Nano Lett.* **12,** 4380–4384 (2012).
26. Jin, R. C. *et al.* Controlling anisotropic nanoparticle growth through plasmon excitation. *Nature* **425,** 487–490 (2003).
27. Reismann, M., Bretschneider, J. C., von Plessen, G. & Simon, U. Reversible photothermal melting of DNA in DNA–gold-nanoparticle networks. *Small* **4,** 607–610 (2008).
28. Jain, P. K., Qian, W. & El-Sayed, M. A. Ultrafast cooling of photoexcited electrons in gold nanoparticle-thiolated DNA conjugates involves the dissociation of the gold–thiol bond. *J. Am. Chem. Soc.* **128,** 2426–2433 (2006).
29. Alper, J., Crespo, M. & Hamad-Schifferli, K. Release mechanism of octadecyl rhodamine B chloride from Au nanorods by ultrafast laser pulses. *J. Phys. Chem. C* **113,** 5967–5973 (2009).
30. Huschka, R. *et al.* Light-induced release of DNA from gold nanoparticles: nanoshells and nanorods. *J. Am. Chem. Soc.* **133,** 12247–12255 (2011).

Acknowledgements

The authors acknowledge funding support from the National Science Foundation (NSF; grant no. DMR-1344290) and the NSF Materials World Network (grant no. DMR-1210170). The authors also acknowledge facility support from Molecule Foundry at LBNL.

Author contributions

S.Y. performed experiments and measurements. S.Y. and B.K. contributed the numerical simulations. S.Y. and X.N. performed the angle-resolved scattering experiment and X.N. calculated the effective metamaterials properties. S.Y., X.Y. and X.Z. prepared the manuscript. All authors contributed to discussions and manuscript revision. X.Z. guided the research.

Additional information

Supplementary information is available in the online version of the paper. Reprints and permissions information is available online at www.nature.com/reprints. Correspondence and requests for materials should be addressed to X.Z.

Competing financial interests

The authors declare no competing financial interests.